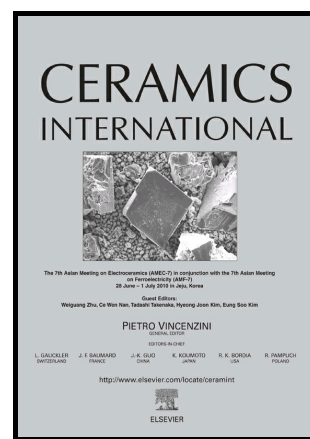


One-Step Fabrication of Surface-Decorated  
Inorganic Nanowires via Single-Nozzle  
Electrospinning

Jin Goo Lee, Ok Sung Jeon, Jae-ha Myung, Yong  
Gun Shul



[www.elsevier.com/locate/ceri](http://www.elsevier.com/locate/ceri)

PII: S0272-8842(18)30858-7  
DOI: <https://doi.org/10.1016/j.ceramint.2018.03.280>  
Reference: CERI17917

To appear in: *Ceramics International*

Received date: 11 January 2018  
Revised date: 21 March 2018  
Accepted date: 31 March 2018

Cite this article as: Jin Goo Lee, Ok Sung Jeon, Jae-ha Myung and Yong Gun Shul, One-Step Fabrication of Surface-Decorated Inorganic Nanowires via Single-Nozzle Electrospinning, *Ceramics International*, <https://doi.org/10.1016/j.ceramint.2018.03.280>

This is a PDF file of an unedited manuscript that has been accepted for publication. As a service to our customers we are providing this early version of the manuscript. The manuscript will undergo copyediting, typesetting, and review of the resulting galley proof before it is published in its final citable form. Please note that during the production process errors may be discovered which could affect the content, and all legal disclaimers that apply to the journal pertain.

# One-Step Fabrication of Surface-Decorated Inorganic Nanowires via Single-Nozzle Electrospinning

Jin Goo Lee<sup>a</sup>, Ok Sung Jeon<sup>b</sup>, Jae-ha Myung<sup>c</sup>, Yong Gun Shul<sup>a</sup>

<sup>a</sup>School of Chemistry, University of St Andrews, St Andrews, Fife, KY16 9ST, UK

<sup>b</sup>Department of Chemical and Bio-molecular Engineering, Yonsei University, 134 Shinchon-dong, Seodaemun-gu, Seoul, 120-749, Republic of Korea

<sup>c</sup>Department of Materials Science and Engineering, Incheon National University, Incheon 22012, Republic of Korea,

## Abstract

One-dimensional heterostructured nanomaterials represent key building blocks for nanotechnologies due to a large number of applications such as electronics, catalysis, drug delivery, and energy storage and conversion devices. Electrospinning has been considered a straightforward and versatile method to prepare inorganic nanowires, but the heterostructured nanowires have been only fabricated by using dual-nozzle or by introducing additional encapsulating step. Here we report one-step fabrication of surface-decorated inorganic nanowires via single-nozzle electrospinning. Although the electrospinning precursor uses one mixed solution containing nickel salt, ceria nanoparticles, and polyvinylpyrrolidone (PVP), the nanowires show a core/shell-like shape. The surface-decorated nanowires consist of nickel shell and ceria core, which exhibits 95.52 % of methane conversion at 600 °C whereas conventional particle-type catalysts have only 60 % at the same temperature in steam reforming.

**Keywords:** electrospinning, Ni/CeO<sub>2</sub>, CH<sub>4</sub> reforming, core-shell, inorganic nanowires

## Introduction

Heterogeneous catalysis is of overriding importance in many areas of the chemical and energy industries. The multi-functionality in catalytic processes highly depends on architectures designed from nanoscale building blocks, which provides new opportunities to improvement of the catalytic performance.[1,2] In recent years, heterostructured nanowires have attracted great attentions in a wide variety of fields such as catalysis, sensing, and energy conversion and storage because they simultaneously satisfy the smallest dimension for efficient transport of electrons or ions and catalytic bifunctionality for each of the two components to provide a necessary but different reactive contribution to the final product.[3-6] Jiang et al. recently reported Pt alloy nanowires for oxygen-reduction reactions (ORR), which leading to high activity and stability by more (111) facets on the surfaces of Pt alloy nanowires.[7] Nakajima et al. reported that CuO/ZnO nanowires achieved great improvements in hydrogen production by methane steam reforming, and showed high durability because of suppressing particle agglomerations in the nanowires.[8] Therefore, the fibrous heterogeneous catalysts showed peculiar properties and high performances for catalytic reactions.[9-11]

Several preparation methods have been developed for nanowire structures such as chemical etching, hydrothermal synthesis, chemical vapor deposition, electrospinning, or gas-solid reaction. Among these processes, an electrospinning technique has been considered a straightforward and versatile method to prepare inorganic nanowires alongside various fabrication methods.[12-16] However, fabricating the surface-decorated nanowires via the electrospinning technique is more complicated than single-structured nanowires. General fabrication process is separated to more than 2 steps: fabricating nanowire cores and then encapsulating them with nano-particles using deposition devices or wet chemical synthesis.[17,18] Coaxial dual-nozzle electrospinning have been recently reported for one-

step fabrication of the surface-decorated inorganic nanowires, but various factors such as surface tension and viscosity should be carefully controlled between different two solutions.[19-22] In recent year, we have reported that the surface-decorated inorganic nanowires via advanced electrospinning and Pechini (AE&P) process is very effective in an energy conversion device.[18] However, the fabrication method is still separated to 2 steps. In this study, we report that one-step fabrication of the surface-decorated Ni/CeO<sub>2</sub> nanowires via single-nozzle electrospinning based on one mixed solution. The prepared nanowires show core/shell-like shapes, large surface area, and high catalytic activity for CH<sub>4</sub> reduction. From these results, the electrospinning based on the particle/salt mixed solution can be a straightforward method to prepare surface-decorated inorganic nanowires for a large number of catalytic applications such as hydrogen production, fuel cell, or batteries.

## Experimental

*Fabrication of the surface-decorated nanowires:* CeO<sub>2</sub> nanoparticles (Sigma Aldrich) were pre-heated at 300 °C for 3 h to remove moistures and organic residues. Poly vinyl pyrrolidone (PVP, Mw ≈ 1,300,000) were dissolved in ethanol under vigorous stirring, and then Ni(NO<sub>3</sub>)<sub>2</sub>·6H<sub>2</sub>O (Sigma Aldrich) was added to the solutions. The solutions were stirred when the Ni precursors were completely dissolved. CeO<sub>2</sub> nanoparticles were added into the solutions, and the sonication was conducted for 1 h. The solutions were stirred for overnight. The suspension was transferred into a syringe with 24 gauge needle connected to the high voltage power supply. The electrospinning condition was as following: about 9 kV applied current voltage, 20 µl/min feed rate of precursor solution using syringe pump and 15 cm distance from spinneret to collector. The fibres were calcined at 500 °C for 2 h in air, and then reduced at 500 °C for 3 h in 5 % H<sub>2</sub>/N<sub>2</sub> atmosphere.

*Characterizations:* The crystal structure of the electrospun Ni-CeO<sub>2</sub> fibres was measured by X-ray diffractometer (XRD) (Rigaku, Miniflex model) with Cu Kα radiation at room

temperature. Field emission scanning electron microscopy (FE-SEM, JEOL, JSM-6701F model) was used to observe microstructures of the electrospun fibres. Field emission transmission electron microscopy (FE-TEM or HRTEM) (JEOL, JEM 2100-F model) was used to distinguish the Ni shell nanoparticles from the CeO<sub>2</sub> core fibres. Temperature-programmed reduction (TPR) of the same weighted sample (0.1g) was packed in a quartz tube and treated at 900 °C for 30 min in 10% CH<sub>4</sub> atmosphere with flow rate as 50 sccm. The heating rate was 10 °C min<sup>-1</sup>. Methane consumption was measured by a thermal conductivity detector (TCD). Steam reforming reactor was operated in CH<sub>4</sub>, H<sub>2</sub>O and N<sub>2</sub> gas atmosphere with the flow rates of 10 sccm, 30 sccm and 40 sccm, respectively. The sample weight was 0.4 g for bulk (GHSV (Gas hourly space velocity) 2000 h<sup>-1</sup>), fibre (GHSV 5000 h<sup>-1</sup>) samples and 2 g for bulk sample (GHSV 5000 h<sup>-1</sup>) which were loaded on the reactor. The samples were pre-treated with H<sub>2</sub> atmosphere at 700 °C with the heating rate of 5 °C min<sup>-1</sup> and retained at 600 °C for 25 h. The reactor outlet was connected to GC (Gas chromatography): an asymmetric thermal conductivity detector (TCD) simultaneously records H<sub>2</sub>, CO<sub>2</sub>, N<sub>2</sub>, and CO, and a flame ionisation detector (FID) measures CH<sub>4</sub>.

## Results and discussion

Polyvinylpyrrolidone (PVP) is typically adsorbed on oxide surfaces, and then acts as a dispersion agent in aqueous medium due to electrostatically repulsive force between PVP chains. It largely depends on the surface charge of oxide particles, molecular weight, and concentration of PVP. The well-dispersed CeO<sub>2</sub> nanoparticles in ethanol can be found when the small amount of PVP was added into the solution as shown in Figure 1a. In the schematic diagram, the CeO<sub>2</sub> nanoparticles may be dispersed by the repulsive force of PVP adsorbed on the CeO<sub>2</sub> surfaces. Normally, the aggregation between colloidal nanoparticles can be avoided by strongly adsorbed stabilizer due to its steric hindrance effect referring to bumper effect of polymers in the colloidal

dispersion.[23] In this study, FT-IR spectra exhibited similar patterns between PVP and CeO<sub>2</sub>/PVP. The peaks of both samples appeared at the wavelength of 1670, 1430, and 1280 cm<sup>-1</sup> which are related to C=O or C-N stretch, CH<sub>2</sub> scissoring vibrations, and CH<sub>2</sub> wag or C-N stretch, respectively.[24] The slight peak shift of the CeO<sub>2</sub>/PVP from 1670 cm<sup>-1</sup> to 1664 cm<sup>-1</sup> may be due to weak adsorption of PVP onto the surfaces of CeO<sub>2</sub> nanoparticles (Figure S1a). This corresponds to the result reported by Si et al.[25] They also reported PVP was weakly adsorbed on the ceria nano-crystals, and acted as a bridge-linking due to its linear structure and multiple coordinating sites such as carbonyls. Figure 1b shows HRTEM and electron diffraction images of the CeO<sub>2</sub>/PVP solution. It was found that the linear-structured PVP molecule links several CeO<sub>2</sub> nanoparticles in about 50-100 nm size simultaneously (Figure S2). Figure 1c shows green-coloured Ni<sup>2+</sup> solution. Liu et al. reported weak interaction between Ni<sup>2+</sup> ions and PVP in ethanol.[26] The reasons for the weak interaction between Ni<sup>2+</sup> ions and PVP are high reduction potential and low reduction degree of Ni species in the absence of seed.[27] In the FT-IR spectra (Figure S1b), the peak shift of the Ni<sup>2+</sup>/PVP from 1670 cm<sup>-1</sup> to 1658 cm<sup>-1</sup> can be observed, which may be attributed to the interaction between carbonyl group of PVP and Ni<sup>2+</sup> ions. The result corresponds well to that of Liu et al. Moreover, the new peak at 1580 cm<sup>-1</sup> appeared in Ni<sup>2+</sup>/PVP solution. We could not clarify the vibration mode of the peak, but suggest that the peak may result from asymmetric carboxylate units of PVP coordinated to Ni<sup>2+</sup> ions or from nickel acetate as the starting salt.[28] The HRTEM image in Figure 1d was considered Ni nanoparticles captured in PVP chains. Thus, we suggest that Ni, CeO<sub>2</sub> nanoparticles and PVP may co-exist in the prepared mixed solution as the schematic diagram in Figure 1.

In the electrospinning principle, the fluid with high viscosity is located on the inside wall of the nozzle tip and released in a form of nanowires by the electric charge generated on the wall of the nozzle tip. Based on the mechanisms, Alexander et al. prepared the core/shell (PMMA/PAN) nanowires by using one mixed solution consisting of polyacrylonitrile (PAN) with high molecular weight and poly(methylmethacrylate) (PMMA) with relatively low molecular weight.[29] The main reason for this is phase separation between PMMA and PAN, but we assume that viscosity derived from molecular weight may have effects on the core/shell form. The viscosity data shows that PVP play a key role in introduction of the viscosity in the solution (Figure S3). Although the viscosity may be same in the solution containing polymer/metal/CeO<sub>2</sub>, but the extra PVP linked with Ni ions may be more favourable to be located on the inside wall of the nozzle tip. When the Ni/PVP is released from the nozzle tip, the dispersed CeO<sub>2</sub> nanoparticles may be carried away by the pulling force of the Ni/PVP. Figure 2b clearly shows that despite of the particle-based electrospinning, the as-electrospun Ni/CeO<sub>2</sub>/PVP nanowires had very smooth surfaces, which implies that the Ni/PVP covered the particle-based CeO<sub>2</sub> nanowires. The nanowire diameter was about 400 nm. Figure 2c shows SEM image of the NiO/CeO<sub>2</sub> nanowires after calcination at 600 °C for 5 h in air. The nanowire diameter was decreased to about 300 nm due to PVP removal. As PVP was removed from the nanowires, the smooth surfaces were changed to the rough surfaces. This may be attributed to NiO nanoparticles on the CeO<sub>2</sub> nanowires. The XRD patterns of the nanowires calcined in air can support above suggestion (Figure S4). Furthermore, the NiO/CeO<sub>2</sub> nanowires maintained the shape of the surface-decorated nanowire even when they were reduced into Ni/CeO<sub>2-δ</sub> nanowires at 500 °C for 3 h in 5 % H<sub>2</sub>/N<sub>2</sub> atmosphere.

The surface-decorated nanowire structures were confirmed by HRTEM as shown in Figure 3. The Ni/CeO<sub>2</sub> nanowires consisted of the Ni shells with about 20-30 nm thickness on CeO<sub>2</sub> core wires (Figure 3a). The Ni nanoparticles were well-distributed on the surfaces of the CeO<sub>2</sub> nanowires. Figure 3b indicates the magnified image and electron diffraction patterns of the shells, which clearly demonstrates that the shells were Ni nanoparticles. In Figure 3c, the line profile data shows the small amount of Ni nanoparticles was contained inside the CeO<sub>2</sub> nanowires. This may be due to PVP adsorbed on the surfaces of the CeO<sub>2</sub> nanoparticles in preparation of the CeO<sub>2</sub>/PVP solution. It proves that the surface-decorated nanowires can be formed via single-nozzle electrospinning based on the one mixed Ni/CeO<sub>2</sub> solution although they were not perfectly symmetrical core/shell nanowires. The amount of Ni loading was about 15 wt.% as shown in Figure S5.

To estimate the catalytic activities of the Ni/CeO<sub>2</sub> bulk and fibres and understand the differences between the two, CH<sub>4</sub>-TPR and steam reforming test were conducted to the samples. The initial temperature for CH<sub>4</sub> consumption was around 400 °C in the Ni-decorated CeO<sub>2</sub> fibres and 580 °C in the Ni/CeO<sub>2</sub> bulk (Figure 4a) which indicates that the Ni-decorated CeO<sub>2</sub> fibres can improve CH<sub>4</sub> reductions at lower temperatures. Additionally, the peak area was larger in the Ni-decorated CeO<sub>2</sub> fibres than in the bulk samples, which indirectly implies higher CH<sub>4</sub> reductions in the former. To conduct precise comparative analysis of CH<sub>4</sub> conversion between bulk and Ni-decorated CeO<sub>2</sub> fibre samples, two identical conditions, GHSV and weight, were considered. The results of steam reforming tests showed significant difference between two samples. Methane was consumed averagely 95.52 % on Ni-decorated CeO<sub>2</sub> fibres, but the bulk samples showed below 60 %. Fibrous structure was not adversely affected by mass transfer which results in the stable operation for 25 h. It was strong point of fibrous



structure to steam reforming which simplifies the catalyst preparation process because it probably skips the pelleting process.

## Conclusions

We prepared the Ni-decorated CeO<sub>2</sub> fibres via single-nozzle electrospinning. The interactions among PVP/Ni/CeO<sub>2</sub> can produce core-shell like fibres spontaneously. The fibres showed high specific surface area and possibility for improvements in CH<sub>4</sub> reductions at low temperatures. Thus, we suggest that this technique and theoretical backgrounds may be helpful for easy preparation of metal-decorated ceramic nanowires, which can extend a variety of applications in energy or catalytic fields.

## Acknowledgements

This research was supported by Basic Science Research Program through the National Research Foundation of Korea (NRF) funded by the Ministry of Education (NRF-2017R1A6A3A03004416) and (NRF-2015M1A2A2056833).

## References

1. D. Wang, C. M. Lieber, Inorganic materials: Nanocrystals branch out. *Nat. Mater.*, 2 (2003) 355
2. D. R. Rolison Catalytic nanoarchitectures--the importance of nothing and the unimportance of periodicity. *Science.*, 229 (2003) 1698
3. A. S. Arico, P. Bruce, B. Scrosati, J. Tarascon, W. V. Schalkwi, Nanostructured materials for advanced energy conversion and storage devices. *Nat. Mater.* 4 (2005) 366.
4. D. Lin, H. Wu, R. Zhang, W. Pan, Enhanced Photocatalysis of Electrospun Ag-ZnO Heterostructured Nanofibers. *Chem. Mater.* 21 (2009) 3479-3484.
5. R. Yan, D. Gargas, P. Yang, Nanowire photonics. *Nature Photon.* 3 (2009) 569-576.

6. Z. Chen, D. Cummins, B. N. Reinecke, E. Clark, M. K. Sunkara, T. F. Jaramillo, Core-shell  $\text{MoO}_3$ - $\text{MoS}_2$  Nanowires for Hydrogen Evolution: A Functional Design for Electrocatalytic Materials. *Nano Lett.* 11 (2011) 4168-4175.
7. K. Jiang, D. Zhao, S. Guo, X. Zhang, X. Zhu, J. Guo, G. Lu and X. Huang, Efficient oxygen reduction catalysis by subnanometer Pt alloy nanowires. *Science Advances* 3 (2017) e1601705
8. H. Nakajima, D. Lee, M.-T. Lee, C. P. Grigoropoulos, Hydrogen production with  $\text{CuO}/\text{ZnO}$  nanowire catalyst for a nanocatalytic solar thermal steam-methanol reformer. *J. Int. Hydrogen Energ.* 41 (2016) 16927-16931
9. Y. K. Mishra, R. Adelung,  $\text{ZnO}$  tetrapod materials for functional applications. In press (2017) DOI:10.1016/j.mattod.2017.11.003
10. A. Nasajpour et al. Nanostructured Fibrous Membranes with Rose Spike-Like Architecture. 17 (2017) 6235–6240
11. J. Gröttrup, F. Schütt, D. Smazna, O. Lupan, R. Adelung, Y. K. Mishra, Porous ceramics based on hybrid inorganic tetrapodal networks for efficient photocatalysis and water purification. 43 (2017) 14915-14922
12. J. T. McCann, M. Marquez, Y. Xia, Melt Coaxial Electrospinning: A Versatile Method for the Encapsulation of Solid Materials and Fabrication of Phase Change Nanofibers. *Nano Lett.* 6 (2006) 2868-2872.
13. Z. Dong, S. J. Kennedy, Y. Wu, Electrospinning materials for energy-related applications and devices. *J. Power Sources* 196 (2011) 196, 4886-4904.
14. J. Hu, T. W. Odom, C. M. Lieber, Chemistry and Physics in One Dimension: Synthesis and Properties of Nanowires and Nanotubes. *Acc. Chem. Res.* 32 (1999) 435-445.

15. T. Subbiah, G. S. Bhat, R. W. Tock, S. Parameswaran, S. S. Ramkumar, Electrospinning of nanofibers. *J. Appl. Polym. Sci.* 96 (2005) 557-569.
16. Greiner A.; Wendorff J. H. Electrospinning: A Fascinating Method for the Preparation of Ultrathin Fibers. *Angew. Chem. Int. Ed.* 46 (2007) 5670-5703.
17. Kayaci F.; Vempati S.; Ozgit-akgun C.; Donmez I.; Biyikli N.; Uyar T. Selective isolation of the electron or hole in photocatalysis: ZnO–TiO<sub>2</sub> and TiO<sub>2</sub>–ZnO core–shell structured heterojunction nanofibers via electrospinning and atomic layer deposition. *Nanoscale* 6 (2014) 5735-5745.
18. Lee J. G.; Park J. H.; Shul Y. G. Tailoring gadolinium-doped ceria-based solid oxide fuel cells to achieve 2 W cm<sup>-2</sup> at 550 °C. *Nat. Commun.* 5, (2014) 4045, DOI:10.1038/ncomms5045.
19. Peng X.; Santulli A. C.; Sutter E.; Wong S. S. Fabrication and enhanced photocatalytic activity of inorganic core–shell nanofibers produced by coaxial electrospinning. *Chem. Sci.*, 3 (2012) 1262-1272.
20. Zhou X.; Shang C.; Gu L.; Dong S.; Chen X.; Han P.; Li L.; Yao J.; Liu Z.; Xu H.; Zhu Y.; Cui G. Facile Preparation of Mesoporous Titanium Nitride Microspheres for Electrochemical Energy Storage. *ACS Appl. Mater. Interfaces* 3 (2011) 3058-3063.
21. Hwang T. H.; Lee Y. M.; Kong B.; Seo J.; Choi J. W. Electrospun Core–Shell Fibers for Robust Silicon Nanoparticle-Based Lithium Ion Battery Anodes. *Nano Lett.* 12 (2012) 802-807.
22. Sun Z.; Zussman E.; Yarin A. L.; Wendorff J. H.; Greiner A. Compound Core–Shell Polymer Nanofibers by Co-Electrospinning. *Adv. Mater.* 2003, 15, 1929-1932.
23. Spalla O.; Nabavi M.; Minter J.; Cabane B. Osmotic compression of mixtures of polymers and particles. *Colloid Polym. Sci.* 274 (1996) 555-567.

24. Borodko Y.; Habas S. E.; Koebel M.; Yang P.; Frei H.; Somorjai G. A. Probing the Interaction of Poly(vinylpyrrolidone) with Platinum Nanocrystals by UV–Raman and FTIR. *J. Phys. Chem. B* 110 (2006) 23052-23059.
25. Si R.; Zhang Y.; You L.; Yan C. Self-Organized Monolayer of Nanosized Ceria Colloids Stabilized by Poly(vinylpyrrolidone). *J. Phys. Chem. B* 110, (2006) 5994-6000.
26. Liu M.; Yan X.; Liu H.; Yu W. An investigation of the interaction between polyvinylpyrrolidone and metal cations. *React Funct. Polym.* 44, (2000) 55-64
27. Barret K.E. Dispersion polymerisation in organic media. *J. Br. Polym. J.* 5, (1973) 259-271
28. Georgakilas V.; Tzitzios V.; Gournis D.; Petridis D. Attachment of Magnetic Nanoparticles on Carbon Nanotubes and Their Soluble Derivatives. *Chem. Mater.* 17, (2005) 1613-1617
29. Bazilevsky A. V.; Yarin A. L.; Megaridis C. M. Co-electrospinning of Core–Shell Fibers Using a Single-Nozzle Technique. *Langmuir*, 23 (5), (2007) 2311–2314

**Figure 1.** Preparation process of the mixed solution consisting of CeO<sub>2</sub> nanoparticles, Ni<sup>2+</sup> ions, polyvinylpyrrolidone (PVP), and ethanol. (a) real image of the well-dispersed CeO<sub>2</sub> nanoparticles by the small amount of PVP and the corresponding schematic diagram, (b) real image of the Ni<sup>2+</sup> solution and the corresponding schematic diagram, (c) HRTEM and electron diffraction images (inset) of the CeO<sub>2</sub> solution. The CeO<sub>2</sub> nanoparticles are surrounded by PVP, and the electron diffraction image of the dark black particles corresponds

to the crystal structure of  $\text{CeO}_2$ . (d) HRTEM and electron diffraction images (inset) of the  $\text{Ni}^{2+}$  solution, showing Ni particle captured in PVP chains.

**Figure 2.** Electrospinning processes based on the mixed solution and the corresponding SEM and HRTEM images to each step. (a) schematic diagram of the electrospinning using the mixed solution. The polymer/metal ions with high viscosity may be located on the inside wall of the nozzle tip, and the  $\text{CeO}_2$  nanoparticles with relatively low viscosity may move out to the entrance of the nozzle tip by pulling force. (b) SEM image of the as-electrospun  $\text{Ni/CeO}_2$  nanowire, showing the fine surfaces of the nanowire despite of the particle-based electrospinning. (c) SEM image of the calcined nanowires in air.  $\text{NiO}$  nanoparticles appear on the  $\text{CeO}_2$  nanowires. (d) schematic diagram and HRTEM image of the  $\text{Ni/CeO}_2$  nanowire after heat treatment in reducing atmosphere.

**Figure 3.** HRTEM images of the  $\text{Ni/CeO}_2$  nanowires after heat treatment in reducing atmosphere. (a) HRTEM image of the  $\text{Ni/CeO}_2$  nanowire surfaces, (b) magnified image of the Ni shells and electron diffraction image (inset) clearly shows the crystal structure of Ni. (c) line profile data of the  $\text{Ni/CeO}_2$  nanowire, showing the core/shell-like structure.

**Figure 4.** (a)  $\text{CH}_4$  TPR signals of the  $\text{Ni/CeO}_2$  particle mixtures (bulk) and nanowires (fiber) after heat treatment in reducing atmosphere. (b) Methane conversion of the  $\text{Ni/CeO}_2$  particle mixtures and nanowires with steam reforming condition at 600 °C.

Figure 1.

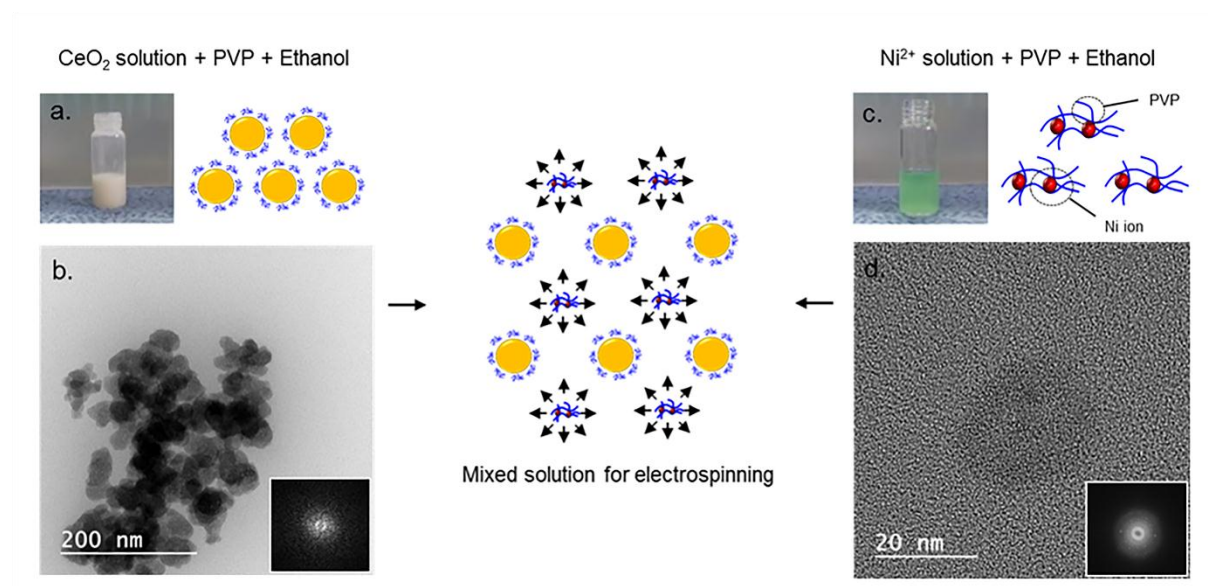


Figure 2.

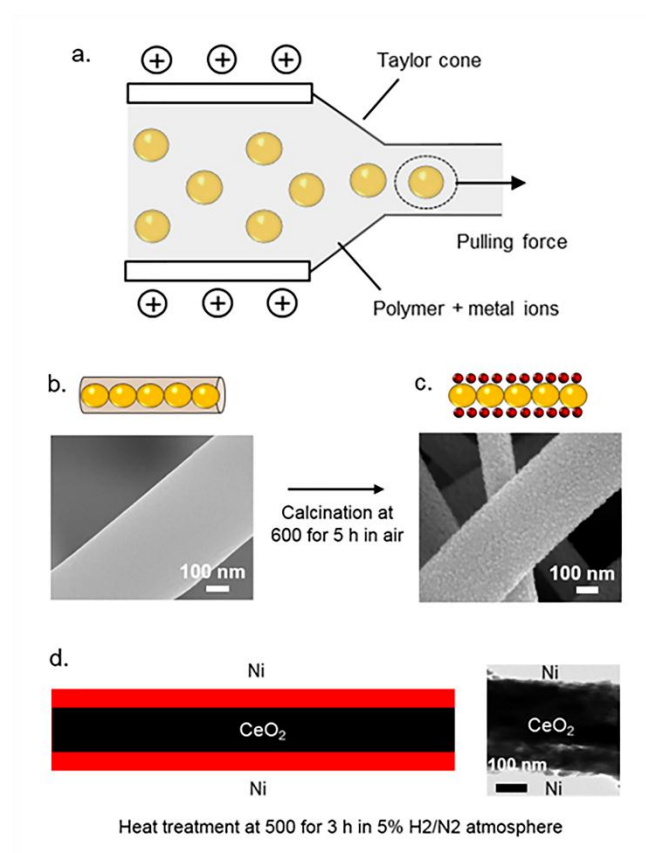


Figure 3.

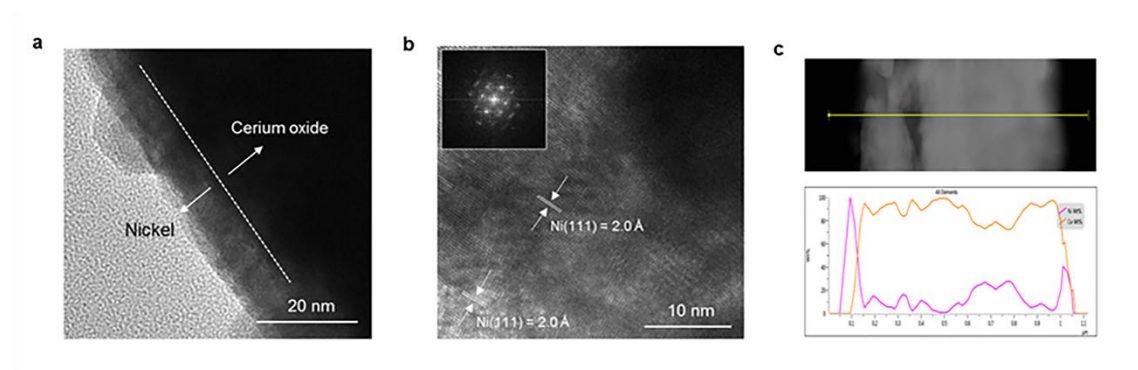




Figure 4.

